



ISSN: 0067-2904
GIF: 0.851

Effects of rotation and MHD on the Nonlinear Peristaltic Flow of a Jeffery Fluid in an Asymmetric Channel through a Porous Medium

Ahmad M. Abdulhadi, Aya H. Al-Hadad*

Department of Mathematics, Collage of Science, University of Baghdad, Baghdad, Iraq

Abstract

In this paper, the effect of both rotation and magnetic field on peristaltic transport of Jeffery fluid through a porous medium in a channel are studied analytically and computed numerically. Mathematical modeling is carried out by utilizing long wavelength and low Reynolds number assumptions. Closed form expressions for the pressure gradient, pressure rise, stream function, velocity and shear stress on the channel walls have been computed numerically. Effects of Hartman number, time mean flow, wave amplitude, porosity and rotation on the pressure gradient, pressure rise, stream function, velocity and shear stress are discussed in detail and shown graphically. The results indicate that the effect of Hartman number, time mean flow, wave amplitude, porosity and rotation are very pronounced in the phenomena, when we change a Jeffery fluid to second order fluid we obtain the results of [1].

Keywords: Peristaltic flow, Jeffery fluid, Magnetic field, Porous medium.

تأثير التدوير والمجال المغناطيسي الهيدروديناميكي على الجريان التاموجي الغير خطي لمائع جيفري في قناة متمائلة خلال وسط مسامي

أحمد مولود عبد الهادي، آية هادي الحداد*

قسم الرياضيات، كلية العلوم، جامعة بغداد، بغداد، العراق

الخلاصة

في هذا البحث، تأثير كلا من التدوير والمجال المغناطيسي على الانتقال التاموجي لمائع جيفري خلال وسط مسامي في القناة تم دراسته تحليلياً وحسابه عددياً. وتتم النمذجة الرياضية من خلال فرضيات طول الموجة و عدد رينولد قليل. تم احتساب تعبيرات شكل المغلقة ل انحدار الضغط، ارتفاع الضغط، ودالة التدفق، السرعة وقوة التشوه المؤثره على جدران القناة عددياً. تأثير كلا من عدد هارتمان، معدل الجريان للزمن، سعة الموجه، المسامية والتدوير على كلا من انحدار للضغط وارتفاع الضغط، دالة التدفق، السرعة و قوة التشوه قد نوقشت بالتفاصيل ومبينه بالرسوم. النتائج تشير الى ان تأثير عدد هارتمان، معدل الجريان للزمن، سعة الموجه، المسامية والتدوير واضح جدا في هذه الظاهرة. وعندما نقوم بتبديل المائع من جيفري الى مائع من الدرجة الثانية نحصل على نفس النتائج المذكورة في [1].

1. Introduction

Flows through porous medium occur in filtration of fluids and seepage of water in river beds. Movement of underground, water and oils are some important examples of flows through porous medium. Ann oil reservoir mostly contains of sedimentary formation such as limestone and sandstone in which oil is entrapped. Another example of flow through porous medium is the seepage under a dam which is very important. There are examples of neutral porous medium such as beach sand, rye bread.

*Email: ayaalhadad@yahoo.com

The physics of flow through a porous media discussed by Scheidgger, A.E [2], Srinivas, S. and Gayathri, R. [3] have studied peristaltic transport of a Newtonian fluid in a vertical asymmetric channel with heat transfer and porous medium, Kothandapani, M. and Srinivas, S. [4] have studied peristaltic transport of a Jeffery fluid under the effect of magnetic field in an asymmetric channel, Mahmoud S. R., Afifi N. A. S. and Al-Isede H. M., [5] have studied effect of porous medium and magnetic field on the peristaltic transport of a Jeffery fluid, Abd-Alla A.M. and Abo-Dahab S.M., [6] have studied magnetic field and rotation effects on the peristaltic transport of a Jeffery fluid in an asymmetric channel, Nadeem S., Arshad riaz and Ellahi R., [7] have studied peristaltic flow of a Jeffery fluid in rectangular duct having compliant walls. Mahmoud S.R., Abd-alla A.M. and El-sheikh M.A., [8] discussed the effect of the rotation on wave motion through cylindrical bore in a micro-polar porous medium.

The aim of the paper is to discuss the peristaltic flow of Jeffery fluid through a porous medium in a two-dimensional channel. The governing equation is modeled and then solved analytically within the long wavelength and low Reynolds number approximation. The pressure gradient, stream function, pressure rise, friction force, shear stress and velocity to observe the effect of the Hartman number, time-mean flow, wave amplitude, porosity and rotation on the peristaltic motion of a Jeffery fluid. Numerical calculations are carried out and illustrated graphically in each case considered.

2. Basic equations

The basic vector equations governing the flow of a Jeffery fluid through a porous medium in a rotation frame are:

$$\bar{\nabla} \cdot \bar{V} = 0 \quad (1)$$

$$\rho \frac{D\bar{V}}{Dt} + \rho \left[\bar{\Omega} \times (\bar{\Omega} \times \bar{V}) + 2\bar{\Omega} \times \frac{\partial \bar{V}}{\partial t} \right] = \bar{\nabla} \cdot \bar{T} - \frac{\mu}{K} \bar{V} + \rho \bar{f} - eP_0^2 \bar{U} \quad (2)$$

Where ρ is the density, $\bar{\Omega} = \bar{\Omega}k$, k is the unit vector parallel to z axis, $\bar{\Omega}$ is the rotation, \bar{V} is the velocity vector, \bar{K} is the permeability of the porous medium, \bar{f} is the body force, e is the coefficient of electrical conductivity, P_0 is the magnetic field, $\frac{D}{Dt}$ denote the material derivative and

\bar{T} is the Cauchy stress tensor. The constitutive equation for an incompressible Jeffery fluid can be expressed as [6]

$$\bar{T} = -\bar{p}\bar{I} + \bar{S} \quad (3)$$

Where \bar{p} is the pressure, \bar{I} is the identity tensor and \bar{S} is the extra stress for the Jeffrey fluid which is defined as [6]:

$$\bar{S} = \frac{\mu}{1 + \lambda_1} * (\bar{\dot{\gamma}} + \lambda_2 \bar{\ddot{\gamma}}) \quad (4)$$

Where μ is the dynamic viscosity, λ_1 is the ratio of relaxation to retardation times, λ_2 is the retardation time, $\bar{\dot{\gamma}}$ is the shear rate.

Where

$$\bar{\dot{\gamma}} = \nabla \bar{V} + (\nabla \bar{V})^T \quad (5)$$

$$\bar{\ddot{\gamma}} = \frac{D}{Dt} \bar{\dot{\gamma}} = \frac{\partial}{\partial t} \bar{\dot{\gamma}} + (\bar{V} \cdot \nabla) \bar{\dot{\gamma}} \quad (6)$$

Now, substituting (5), (6) in (4), we get

$$\bar{S} = \frac{\mu}{1 + \lambda_1} \left(1 + \lambda_2 \left(\bar{u} \frac{\partial}{\partial x} + \bar{v} \frac{\partial}{\partial y} \right) \right) \bar{\dot{\gamma}} \quad (7)$$

Then the stress component are given by

$$\bar{S}_{xx} = \frac{\mu}{1 + \lambda_1} \left(2\bar{u}_x + 2\lambda_2 \left(\bar{u} \frac{\partial^2 \bar{u}}{\partial x^2} + \bar{v} \frac{\partial^2 \bar{u}}{\partial x \partial y} \right) \right) \quad (8)$$

$$\bar{S}_{xy} = \frac{\mu}{1 + \lambda_1} \left(\bar{v}_x + \bar{u}_y + \lambda_2 \left(\bar{u} \frac{\partial}{\partial x} (\bar{v}_x + \bar{u}_y) + \bar{v} \frac{\partial}{\partial y} (\bar{v}_x + \bar{u}_y) \right) \right) \quad (9)$$

$$\bar{S}_{yy} = \frac{\mu}{1 + \lambda_1} \left(2\bar{v}_y + 2\lambda_2 \left(\bar{u} \frac{\partial^2 \bar{v}}{\partial x \partial y} + \bar{v} \frac{\partial^2 \bar{v}}{\partial y^2} \right) \right) \quad (10)$$

3. Formulation of the problem

Let us consider the peristaltic transport of Jeffery fluid through a porous medium. In the laboratory, we choose the Cartesian coordinates system (\bar{X}, \bar{Y}) for the channel with \bar{X} along the center line \bar{Y} transverse it, the motion of an incompressible viscous Jeffery fluid in a channel induced by sinusoidal wave trains propagating with constant speed c along the channel walls. The geometry of the wall surface is represented by

$$\bar{h}(\bar{X}, \bar{t}) = a + b \sin \frac{2\pi}{\lambda} (\bar{X} - c\bar{t}) \quad (11)$$

Where a is the half width of the channel, b is the wave amplitude, λ is the wave length, c is the propagation velocity and \bar{t} is the time.

We introducing a wave frame (\bar{x}, \bar{y}) moving with velocity c away from the fixed frame (\bar{X}, \bar{Y}) by the transformation:

$$\bar{x} = \bar{X} - c\bar{t}, \quad \bar{y} = \bar{Y}, \quad \bar{u} = \bar{U} - c, \quad \bar{v} = \bar{V}, \quad \bar{p}(\bar{x}) = \bar{P}(\bar{X}, \bar{t}) \quad (12)$$

Where \bar{u} and \bar{v} are the dimensional velocity components in the direction of \bar{x} and \bar{y} , respectively, \bar{p} and \bar{P} are pressures in wave and fixed frame, respectively. The pressure \bar{p} remains a constant across any axial station of the channel under the assumption that the wavelength is large.

In a laboratory frame, the governing equations are reduced to the following form:

$$\frac{\partial \bar{u}}{\partial \bar{x}} + \frac{\partial \bar{v}}{\partial \bar{y}} = 0, \quad (13)$$

$$\rho \left(\bar{u} \frac{\partial \bar{u}}{\partial \bar{x}} + \bar{v} \frac{\partial \bar{u}}{\partial \bar{y}} \right) - \rho \Omega \left(\Omega \bar{u} + 2 \frac{\partial \bar{v}}{\partial \bar{t}} \right) = - \frac{\partial \bar{p}}{\partial \bar{x}} + \frac{\partial \bar{S}_{xx}}{\partial \bar{x}} + \frac{\partial \bar{S}_{xy}}{\partial \bar{y}} - \frac{\mu}{K} (\bar{u} + c) - eP_0^2 (\bar{u} + c), \quad (14)$$

$$\rho \left(\bar{u} \frac{\partial \bar{v}}{\partial \bar{x}} + \bar{v} \frac{\partial \bar{v}}{\partial \bar{y}} \right) - \rho \Omega \left(\Omega \bar{v} - 2 \frac{\partial \bar{u}}{\partial \bar{t}} \right) = - \frac{\partial \bar{p}}{\partial \bar{y}} + \frac{\partial \bar{S}_{xy}}{\partial \bar{x}} + \frac{\partial \bar{S}_{yy}}{\partial \bar{y}} - \frac{\mu}{K} \bar{v}. \quad (15)$$

Introduce the following non-dimensional variable and parameters [2]:

$$x = \frac{\bar{x}}{\lambda}, \quad y = \frac{\bar{y}}{a}, \quad u = \frac{\bar{u}}{c}, \quad v = \frac{\bar{v}}{c}, \quad p = \frac{a^2 \bar{p}}{c \lambda \mu}, \quad S = \frac{a \bar{S}}{\mu c}, \quad t = \frac{c \bar{t}}{\lambda}, \quad h = \frac{\bar{h}}{a}, \quad \phi = \frac{b}{a}, \quad \delta = \frac{a}{\lambda}, \quad \sigma^2 = \frac{a^2}{K},$$

$$\text{Re} = \frac{ca\rho}{\mu}, \quad M = \sqrt{\frac{e}{\mu} a P_0}. \quad (16)$$

Where ϕ is the amplitude ratio, δ is the dimensionless wave number, σ^2 is the porosity, parameter, Re is the Reynolds number, M is the Hartman number.

By using Eqs. (16) and (12) and introducing the dimensionless stream function $\psi(x, y)$ such that:

$$u = \frac{\partial \psi}{\partial y}, \quad v = -\delta \frac{\partial \psi}{\partial x} \quad (17)$$

and eliminating the pressure gradient we obtain:

$$\text{Re} \delta \left(\frac{\partial \psi}{\partial y} \frac{\partial^2 \psi}{\partial x \partial y} - \frac{\partial \psi}{\partial x} \frac{\partial^2 \psi}{\partial y^2} \right) - \left(\frac{\rho a^2 \Omega^2}{\mu} \frac{\partial \psi}{\partial y} - 2 \delta^2 \text{Re} \Omega \frac{\partial^2 \psi}{\partial t \partial x} \right) =$$

$$\delta \frac{\partial}{\partial x} \left(\frac{2\delta}{1 + \lambda_1} \left(\frac{\partial^2 \psi}{\partial x \partial y} + \frac{c \lambda_2}{\lambda} \left(\frac{\partial^4 \psi}{\partial x^2 \partial y^2} - \frac{\partial^4 \psi}{\partial x^2 \partial y^2} \right) \right) + \frac{\partial}{\partial y} \left(\left(\frac{1}{1 + \lambda_1} \right) \right) \right)$$

$$\left(\delta + \frac{\delta}{\lambda} c \lambda_2 \left(\frac{\partial \psi}{\partial y} \frac{\partial}{\partial x} - \frac{\partial \psi}{\partial x} \frac{\partial}{\partial y}\right)\right) \left(\frac{\partial^2 \psi}{\partial y^2} - \delta^2 \frac{\partial^2 \psi}{\partial x^2}\right) - \sigma^2 \left(\frac{\partial \psi}{\partial y} + 1\right) - M^2 \left(\frac{\partial \psi}{\partial y} + 1\right) \tag{18}$$

$$\begin{aligned} & \text{Re } \delta^2 \left(-\delta \frac{\partial^3 \psi}{\partial y \partial^2 x} - \frac{\partial^3 \psi}{\partial y \partial^2 x}\right) - \delta \left(-\delta \frac{\rho a^2 \Omega^2}{\mu} \frac{\partial \psi}{\partial x} - 2\delta \text{Re } \Omega \frac{\partial^2 \psi}{\partial t \partial y}\right) = \\ & \delta^2 \frac{\partial}{\partial x} \left(\left(\frac{1}{1+\lambda_1}\right) \left(\delta + \frac{\delta}{\lambda} c \lambda_2 \left(\frac{\partial \psi}{\partial y} \frac{\partial}{\partial x} - \frac{\partial \psi}{\partial x} \frac{\partial}{\partial y}\right)\right) \left(\frac{\partial^2 \psi}{\partial y^2} - \delta^2 \frac{\partial^2 \psi}{\partial x^2}\right)\right) \\ & + \delta \frac{\partial}{\partial y} \left(\frac{2\delta}{1+\lambda_1} \left(-\frac{\partial^2 \psi}{\partial y \partial x} + \frac{\lambda_2 c}{\lambda} \left(-\frac{\partial \psi}{\partial y} \frac{\partial^3 \psi}{\partial x^2 \partial y} + \frac{\partial \psi}{\partial x} \frac{\partial^3 \psi}{\partial y^2 \partial x}\right)\right)\right) + \sigma^2 \delta^2 \frac{\partial \psi}{\partial x} \end{aligned} \tag{19}$$

With low δ using the long wavelength approximation and neglecting the wave along number Reynolds number in our analysis, then Eqs.(18) and (19) becomes:

$$0 = \frac{\partial}{\partial y} \left(\frac{1}{1+\lambda_1} \left(\frac{\partial^2 \psi}{\partial y^2}\right)\right) - \sigma^2 \left(\frac{\partial \psi}{\partial y} + 1\right) - M^2 \left(\frac{\partial \psi}{\partial y} + 1\right) + \frac{\rho a^2 \Omega^2}{\mu} \frac{\partial \psi}{\partial y} \tag{20}$$

4. Boundary conditions

The boundary conditions for the stream functions in the wave frame as given in [1]:

$$\begin{aligned} \psi = 0, \quad \frac{\partial^2 \psi}{\partial y^2} = 0 \quad \text{at, } y = 0, \\ \psi = F, \quad \frac{\partial \psi}{\partial y} = -1, \quad \text{at } y = h(x) = 1 + \phi \sin(2\pi x) \end{aligned} \tag{21}$$

5. Solution of the problem

Differentiating eq. (20), let $g = \sigma^2 + M^2 - \frac{\rho a^2 \Omega^2}{\mu}$ then Eq. become:

$$\frac{\partial^2}{\partial y^2} \left(\frac{1}{1+\lambda_1} \frac{\partial^2 \psi}{\partial y^2}\right) - g \frac{\partial^2 \psi}{\partial y^2} = 0 \tag{22}$$

By using boundary conditions the solution of equation (21) is

$$\begin{aligned} \psi = & \left(F \sqrt{g} y (1+\lambda_1) \text{Cosh} \left[\sqrt{g} h(x) \sqrt{1+\lambda_1} \right] + \sqrt{1+\lambda_1} \left(y \text{Sinh} \left[\sqrt{g} h(x) \sqrt{1+\lambda_1} \right] - \right. \right. \\ & \left. \left. (F + h(x)) \text{Sinh} \left[\sqrt{g} y \sqrt{1+\lambda_1} \right] \right) \right) / \left(\sqrt{g} h(x) (1+\lambda_1) \text{Cosh} \left[\sqrt{g} h(x) \sqrt{1+\lambda_1} \right] \right. \\ & \left. - \sqrt{1+\lambda_1} \text{Sinh} \left[\sqrt{g} h(x) \sqrt{1+\lambda_1} \right] \right). \end{aligned} \tag{23}$$

By using Eq. (23), we obtain:

$$\begin{aligned} u = & \left(\sqrt{g} (1+\lambda_1) \left(F \text{Cosh} \left[\sqrt{g} h(x) \sqrt{1+\lambda_1} \right] - (F + h(x)) \text{Cosh} \left[\sqrt{g} y \sqrt{1+\lambda_1} \right] \right) + \sqrt{1+\lambda_1} \right. \\ & \left. \text{Sinh} \left[\sqrt{g} h(x) \sqrt{1+\lambda_1} \right] \right) / \left(\sqrt{g} h(x) (1+\lambda_1) \text{Cosh} \left[\sqrt{g} h(x) \sqrt{1+\lambda_1} \right] - \sqrt{1+\lambda_1} \right. \\ & \left. \text{Sinh} \left[\sqrt{g} h(x) \sqrt{1+\lambda_1} \right] \right). \end{aligned} \tag{24}$$

The non-dimensional shear stress is

$$S_{xy} = \frac{1}{1+\lambda_1} \frac{\partial^2 \psi}{\partial y^2} = \left(g(F+h(x))\sqrt{1+\lambda_1} \operatorname{Sinh} \left[\sqrt{g} y \sqrt{1+\lambda_1} \right] \right) / \left(-\sqrt{g} h(x)(1+\lambda_1) \right. \\ \left. \operatorname{Cosh} \left[\sqrt{g} h(x)\sqrt{1+\lambda_1} \right] + \sqrt{1+\lambda_1} \operatorname{Sinh} \left[\sqrt{g} h(x)\sqrt{1+\lambda_1} \right] \right). \quad (25)$$

6. The pressure gradient

Using Eqs.(16) and (12) and introducing the stream function from Eq. (17) and using the along with low Reynolds number δ long wavelength approximation and neglecting the wave on Eqs. (17) - (22), we get:

$$0 = -\frac{\partial p}{\partial x} + \frac{\partial}{\partial y} \left(\frac{1}{1+\lambda_1} \frac{\partial^2 \psi}{\partial y^2} \right) - \sigma^2 \left(\frac{\partial \psi}{\partial y} + 1 \right) - M^2 \left(\frac{\partial \psi}{\partial y} + 1 \right) + \frac{\rho a^2 \Omega^2}{\mu} \frac{\partial \psi}{\partial y} \quad (26)$$

$$0 = -\frac{\partial p}{\partial y} \quad (27)$$

Now, by using Eq. (23) the solution of Eq. (26) is:

$$\frac{dp}{dx} = \left(-\sqrt{g} (1+\lambda_1) \left((F+h(x))\mu(M^2 + \sigma^2) - a^2 F \rho \Omega^2 \right) \operatorname{Cosh} \left[\sqrt{g} h(x)\sqrt{1+\lambda_1} \right] \right. \\ \left. - \sqrt{g} (F+h(x))(1+\lambda_1) (g\mu - \mu(M^2 + \sigma^2) + a^2 \rho \Omega^2) \operatorname{Cosh} \left[\sqrt{g} y \sqrt{1+\lambda_1} \right] + \right. \\ \left. a^2 \sqrt{1+\lambda_1} \rho \Omega^2 \operatorname{Sinh} \left[\sqrt{g} h(x)\sqrt{1+\lambda_1} \right] \right) / \left(\mu (\sqrt{g} h(x)(1+\lambda_1) \right. \\ \left. \operatorname{Cosh} \left[\sqrt{g} h(x)\sqrt{1+\lambda_1} \right] - \sqrt{1+\lambda_1} \operatorname{Sinh} \left[\sqrt{g} h(x)\sqrt{1+\lambda_1} \right] \right) \right). \quad (28)$$

7. Special case

If the porosity parameter is neglected i.e., ($\sigma^2 = 0$), we obtain the following results:

$$\psi = - \left(F y (1+\lambda_1) (M^2 \mu - a^2 \rho \Omega^2) \operatorname{Cosh} \left[\frac{h(x)\sqrt{1+\lambda_1} \sqrt{M^2 \mu - a^2 \rho \Omega^2}}{\sqrt{\mu}} \right] + \sqrt{1+\lambda_1} \sqrt{\mu} \right. \\ \left. \sqrt{M^2 \mu - a^2 \rho \Omega^2} \left(y \operatorname{Sinh} \left[\frac{h(x)\sqrt{1+\lambda_1} \sqrt{M^2 \mu - a^2 \rho \Omega^2}}{\sqrt{\mu}} \right] - (F+h(x)) \right. \right. \\ \left. \left. \operatorname{Sinh} \left[\frac{y \sqrt{1+\lambda_1} \sqrt{M^2 \mu - a^2 \rho \Omega^2}}{\sqrt{\mu}} \right] \right) \right) / \left(-h(x)(1+\lambda_1) (M^2 \mu - a^2 \rho \Omega^2) \right. \\ \left. \operatorname{Cosh} \left[\frac{h(x)\sqrt{1+\lambda_1} \sqrt{M^2 \mu - a^2 \rho \Omega^2}}{\sqrt{\mu}} \right] + \sqrt{1+\lambda_1} \sqrt{\mu} \sqrt{M^2 \mu - a^2 \rho \Omega^2} \right. \\ \left. \operatorname{Sinh} \left[\frac{h(x)\sqrt{1+\lambda_1} \sqrt{M^2 \mu - a^2 \rho \Omega^2}}{\sqrt{\mu}} \right] \right) \quad (29)$$

$$\frac{dp}{dx} = \left(-(1 + \lambda_1)(M^2 \mu - a^2 \rho \Omega^2) \left((F + h(x))M^2 \mu - a^2 F \rho \Omega^2 \right) \right. \\ \left. \text{Cosh} \left[\frac{h(x) \sqrt{1 + \lambda_1} \sqrt{M^2 \mu - a^2 \rho \Omega^2}}{\sqrt{\mu}} \right] + a^2 \sqrt{1 + \lambda_1} \sqrt{\mu} \rho \Omega^2 \sqrt{M^2 \mu - a^2 \rho \Omega^2} \right. \\ \left. \text{Sinh} \left[\frac{h(x) \sqrt{1 + \lambda_1} \sqrt{M^2 \mu - a^2 \rho \Omega^2}}{\sqrt{\mu}} \right] \right) / (h(x)(1 + \lambda_1) \mu (M^2 \mu - a^2 \rho \Omega^2)) \\ \left. \text{Cosh} \left[\frac{h(x) \sqrt{1 + \lambda_1} \sqrt{M^2 \mu - a^2 \rho \Omega^2}}{\sqrt{\mu}} \right] - \sqrt{1 + \lambda_1} \mu^{\frac{3}{2}} \sqrt{M^2 \mu - a^2 \rho \Omega^2} \right. \\ \left. \text{Sinh} \left[\frac{h(x) \sqrt{1 + \lambda_1} \sqrt{M^2 \mu - a^2 \rho \Omega^2}}{\sqrt{\mu}} \right] \right). \quad (30)$$

$$u = \left(-F(1 + \lambda_1)(M^2 \mu - a^2 \rho \Omega^2) \text{Cosh} \left[\frac{h(x) \sqrt{1 + \lambda_1} \sqrt{M^2 \mu - a^2 \rho \Omega^2}}{\sqrt{\mu}} \right] + (F + h(x)) \right. \\ \left. (1 + \lambda_1)(M^2 \mu - a^2 \rho \Omega^2) \text{Cosh} \left[\frac{y \sqrt{1 + \lambda_1} \sqrt{M^2 \mu - a^2 \rho \Omega^2}}{\sqrt{\mu}} \right] - \sqrt{1 + \lambda_1} \sqrt{\mu} \right. \\ \left. \sqrt{M^2 \mu - a^2 \rho \Omega^2} \text{Sinh} \left[\frac{h(x) \sqrt{1 + \lambda_1} \sqrt{M^2 \mu - a^2 \rho \Omega^2}}{\sqrt{\mu}} \right] \right) / (-h(1 + \lambda_1)) \\ \left. (M^2 \mu - a^2 \rho \Omega^2) \text{Cosh} \left[\frac{h(x) \sqrt{1 + \lambda_1} \sqrt{M^2 \mu - a^2 \rho \Omega^2}}{\sqrt{\mu}} \right] + \sqrt{1 + \lambda_1} \sqrt{\mu} \right. \\ \left. \sqrt{M^2 \mu - a^2 \rho \Omega^2} \text{Sinh} \left[\frac{h(x) \sqrt{1 + \lambda_1} \sqrt{M^2 \mu - a^2 \rho \Omega^2}}{\sqrt{\mu}} \right] \right). \quad (31)$$

$$S_{xy} = - \left((F + h(x)) \sqrt{1 + \lambda_1} (M^2 \mu - a^2 \rho \Omega^2)^{\frac{3}{2}} \text{Sinh} \left[\frac{y \sqrt{1 + \lambda_1} \sqrt{M^2 \mu - a^2 \rho \Omega^2}}{\sqrt{\mu}} \right] \right) / \\ \left(h(1 + \lambda_1) \sqrt{\mu} (M^2 \mu - a^2 \rho \Omega^2) \text{Cosh} \left[\frac{h(x) \sqrt{1 + \lambda_1} \sqrt{M^2 \mu - a^2 \rho \Omega^2}}{\sqrt{\mu}} \right] - \sqrt{1 + \lambda_1} \right. \\ \left. \mu \sqrt{M^2 \mu - a^2 \rho \Omega^2} \text{Sinh} \left[\frac{h(x) \sqrt{1 + \lambda_1} \sqrt{M^2 \mu - a^2 \rho \Omega^2}}{\sqrt{\mu}} \right] \right). \quad (32)$$

8. The pressure rise and friction force

The pressure rise ΔP_λ and the friction force F_λ for a channel of length L , in their dimensionless forms, are given by:

$$\Delta P_\lambda = \int_0^1 \frac{dp}{dx} dx, \quad (33)$$

$$F_{\lambda} = \int_0^1 -h^2 \frac{dp}{dx} dx. \quad (34)$$

Where, $\frac{dp}{dx}$ is defined in equation (28) and equation (30) (for special case).

9. Results and discussion

Stream function (9.1)

Figures (1-5) show the variation of absolute value of stream function $|\psi|$ with respect to y , which has oscillatory behavior in the whole range of the y -axis, and is reflected and refracted at $y = 0, 0.9$ for different values of porosity σ , Hartman number M , rotation Ω and the dimensionless time-mean flow in the wave frame F except when the effect of non-dimensional wave amplitude ϕ at $y = 0.95$. It is clear that from figures the absolute value of stream function has nonzero value only in the bounded region of space. It observed that the absolute value of stream function decreases with increasing rotation and dimensionless time-mean flow, while it increases with increasing non-dimensional wave amplitude, the porosity and Hartman number. Figures (6-9) show the variation of absolute of stream function $|\psi|$ with respect to y when the porosity σ is neglected and its reflected and refraction for different values of wave amplitude ϕ , Hartman number M , rotation Ω and the dimensionless time-mean flow in the wave frame F . It is clear that from figures the absolute value of stream function has nonzero value only in the bounded region of space. It shown that the absolute value of stream function decreases with increasing dimensionless time-mean flow, while it increases with increasing non-dimensional wave amplitude, Hartman number and rotation.

Pressure gradient (9.2)

Figures (10-14) show the variations of the absolute value of pressure gradient $\left|\frac{dp}{dx}\right|$ with respect to x , which exhibits oscillatory behavior in the whole range of x for different values of non-dimensional wave amplitude ϕ , porosity σ , Hartman number M , rotation Ω and the dimensionless time-mean flow in the wave frame F . It is clear that the pressure gradient $\left|\frac{dp}{dx}\right|$ has nonzero value only in the bounded region of space. It observed that the absolute value of pressure gradient decreases with increasing dimensionless time-mean flow, while it increases with increasing non-dimensional wave amplitude, the porosity, Hartman number and rotation. It is also found that $\left|\frac{dp}{dx}\right|$ intersects when the effect of non-dimensional wave amplitude at $x = 0.5$ decreases ($0 \leq x \leq 0.5$), while increase at ($0.5 \leq x \leq 1$). Figures (15-18) show the variations of the absolute value pressure gradient $\left|\frac{dp}{dx}\right|$ when the porosity σ is neglected. Which has oscillatory behavior in the whole range of the x -axis for different values of the non-dimensional wave amplitude ϕ , Hartman number M , rotation Ω and the dimensionless time-mean flow F in the wave frame. It appears that the pressure gradien has non zero value only in the bounded region of space. It shown that the absolute value of pressure gradient decreases with increasing dimensionless time-mean flow and rotation, while it increases with increasing non-dimensional wave amplitude and Hartman number. It is also found that $\left|\frac{dp}{dx}\right|$ intersects when the effect of non-dimensional wave amplitude at $x = 0.5$ decreases at ($0 \leq x \leq 0.5$), while increase at ($0.5 \leq x \leq 1$).

Shear stress and velocity (9.3)

Figures (19-23) show the variations of the absolute value of shear stress $|S_{xy}|$ with respect to x , which exhibits oscillatory behavior in the whole range of x -axis for different values of non-

dimensional wave amplitude ϕ , porosity σ , Hartman number M , rotation Ω and the dimensionless time-mean flow in the wave frame F . It is clear that the absolute value of shear stress $|S_{xy}|$ has nonzero value only in the bounded region of space. It is observed that the absolute value of shear stress decreases with increasing dimensionless time-mean flow and rotation, while it increases with increasing non-dimensional wave amplitude, the porosity and Hartman number. It is noted that the values of shear stress are very small at $(0.1 \leq x \leq 0.35)$ for the effects of non-dimensional wave amplitude, Hartman number, porosity, rotation and dimensionless time-mean flow in the wave frame. Figures (24-27) show the variations of the absolute value of shear stress $|S_{xy}|$ with respect to x when the porosity σ is neglected, which has oscillatory behavior in the whole range of the x -axis for different values of the non-dimensional of wave amplitude ϕ , Hartman number M , rotation Ω and the dimensionless time-mean flow F . It is clear that the absolute value of shear stress has a nonzero value only in the bounded region of space. It is shown that the absolute value of shear stress decreases with increasing dimensionless time-mean flow and rotation, while it increases with increasing non-dimensional wave amplitude and Hartman number. It is noted that the absolute value of shear stress is very small at $(0.15 \leq x \leq 0.35)$ for the non-dimensional wave amplitude, Hartman number, rotation and the dimensionless time-mean flow, and it approaches the maximum value at $x = 0.75$. Figures (28-32) show the variations of the absolute value of velocity $|u|$ with respect to y , which reveal oscillatory behavior in the whole range of the y -axis, and vanish at $y \approx 1$ for different values of non-dimensional wave amplitude ϕ , porosity σ , Hartman number M , rotation Ω and the dimensionless time-mean flow F in the wave frame. It is clear that the absolute value of velocity $|u|$ has a nonzero value only in the bounded region of space. It is observed that the absolute value of velocity decreases with increasing dimensionless time-mean flow and rotation, while it increases with increasing non-dimensional wave amplitude, the porosity and Hartman number. Figures (33-36) show the absolute value of velocity $|u|$ with respect to y when the porosity σ is neglected. It is clear that the absolute value of the velocity has a nonzero value only in the bounded region of space. It is shown that the absolute value of velocity decreases with increasing dimensionless time-mean flow, rotation and wave amplitude, while it increases with increasing Hartman number.

Pressure rise and friction force (9.4)

Figures (37-44) show the variations of the absolute value of pressure rise $|\Delta P_\lambda|$ and the absolute value of friction force $|F_\lambda|$, respectively, with respect to the dimensionless time-mean flow in the wave frame F . Reflection and refraction occur at $F = -1$ for different values of non-dimensional wave amplitude ϕ , porosity σ , Hartman number M , rotation Ω . It is clear that the absolute value of pressure rise and the absolute value of friction force have a nonzero value only in the bounded region of space. It is observed that the absolute value of pressure rise and the absolute value of friction force decreases with increasing rotation, while it increases with increasing non-dimensional wave amplitude, the porosity and Hartman number. It is found that the absolute value of pressure rise $|\Delta P_\lambda|$ and the absolute value of friction force $|F_\lambda|$, respectively, are reflected within $(-4 \leq F \leq -1)$ and are refracted within $(-1 \leq F \leq 4)$ for all four values of $\phi, \sigma, M^2, \Omega$.

Figures (45-50) show the variations of the absolute value of pressure rise $|\Delta P_\lambda|$ and the absolute value of friction force $|F_\lambda|$, respectively, with respect to the dimensionless time-mean flow in the wave frame F which it reflects and refracts at $F = -1$ for different values of non-dimensional wave amplitude ϕ , Hartman number M and rotation Ω when the porosity σ is neglected. It is clear that from figures the absolute value of pressure rise and the absolute value of friction force have a nonzero value only in the bounded region of space. It is observed that the absolute value of pressure rise and the absolute value of friction force increase with increasing non-dimensional wave amplitude and Hartman number, while they decrease with increasing rotation.

It is found that the absolute value of pressure rise $|\Delta P_\lambda|$ and the absolute value of friction force $|F_\lambda|$, respectively, are reflected within $(-4 \leq F \leq -1)$ and refracted within $(-1 \leq F \leq 4)$ for all three values of ϕ, M, Ω .

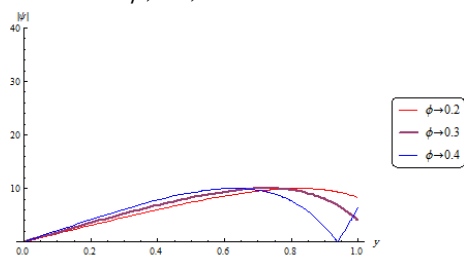


Figure 1-Variation of stream function $|\psi|$ with respect to y for different values of ϕ with other parameters
 $\sigma = 4, M^2 = 5, \Omega = 0.5, F = -10, a = 0.2,$
 $x = 0.7, \mu = 0.4, \rho = 1.057, \lambda_1 = 0.2$

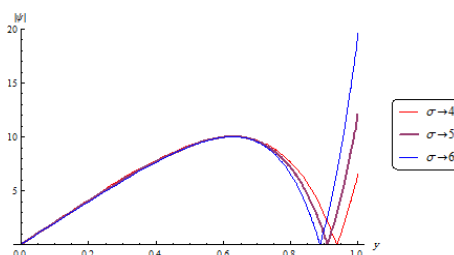


Figure 2-Variation of stream function $|\psi|$ with respect to y for different values of σ with other parameters
 $M^2 = 5, \Omega = 0.5, F = -10, a = 0.2, \phi = 0.2$
 $x = 0.7, \mu = 0.4, \rho = 1.057, \lambda_1 = 0.2$

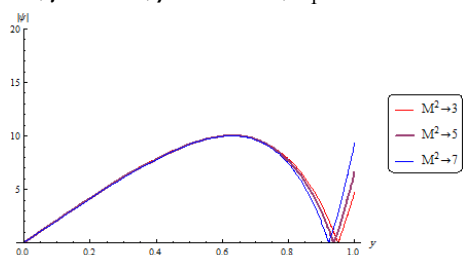


Figure 3-Variation of stream function $|\psi|$ with respect to y for different values of M^2 with other parameters
 $\sigma = 4, \Omega = 0.5, F = -10, a = 0.2, \phi = 0.2$
 $x = 0.7, \mu = 0.4, \rho = 1.057, \lambda_1 = 0.2$

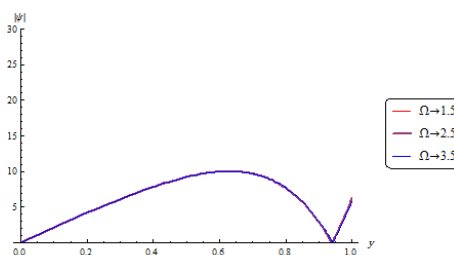


Figure 4-Variation of stream function $|\psi|$ with respect to y for different values of Ω with other parameters
 $M^2 = 5, \sigma = 4, F = -10, a = 0.2, \phi = 0.2$
 $x = 0.7, \mu = 0.4, \rho = 1.057, \lambda_1 = 0.2$

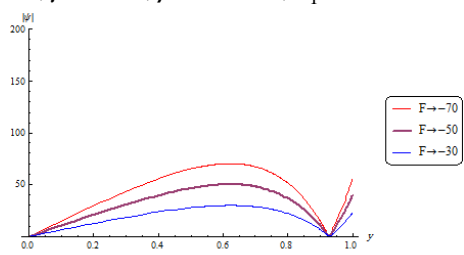


Figure 5-Variation of stream function $|\psi|$ with respect to y for different values of F with other parameters
 $M^2 = 5, \sigma = 4, \Omega = 0.5, a = 0.2, \phi = 0.2$
 $x = 0.7, \mu = 0.4, \rho = 1.057, \lambda_1 = 0.2$

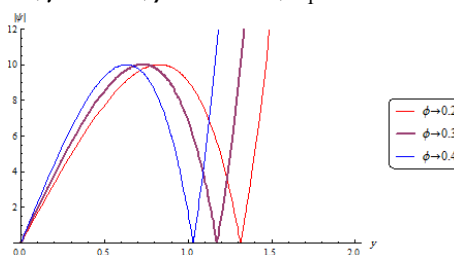


Figure 6-Variation of stream function $|\psi|$ with respect to y for different values of ϕ with other parameters if $(\sigma^2 = 0)$.
 $M^2 = 5, \Omega = 0.5, a = 0.2, F = -10,$
 $x = 0.7, \mu = 0.4, \rho = 1.057, \lambda_1 = 0.2$

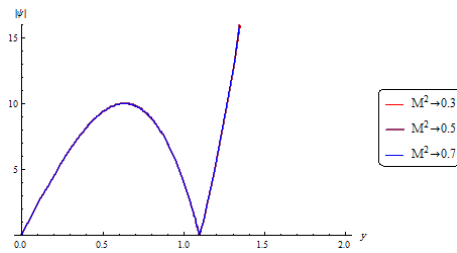


Figure 7-Variation of stream function $|\psi|$ with respect to y for different values of M^2 with other parameters if $(\sigma^2 = 0)$. $\Omega = 0.5, a = 0.2, \phi = 0.2, F = -10$
 $x = 0.7, \mu = 0.4, \rho = 1.057, \lambda_1 = 0.2$

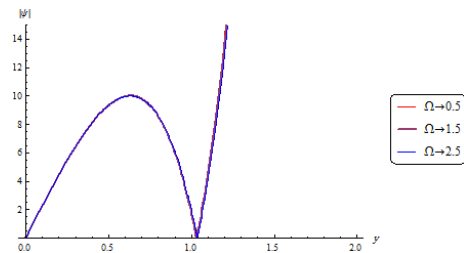


Figure 8-Variation of stream function $|\psi|$ with respect to y for different values of Ω with other parameters if $(\sigma^2 = 0)$. $M^2 = 5, a = 0.2, \phi = 0.4, F = -10$
 $x = 0.7, \mu = 0.4, \rho = 1.057, \lambda_1 = 0.2$

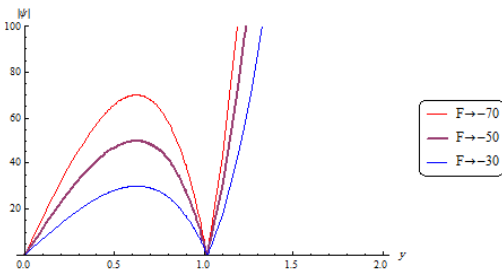


Figure 9-Variation of stream function $|\psi|$ with respect to y for different values of F with other parameters if $(\sigma^2 = 0)$. $M^2 = 5, a = 0.2, \phi = 0.4, \Omega = 0.5$,
 $x = 0.7, \mu = 0.4, \rho = 1.057, \lambda_1 = 0.2$

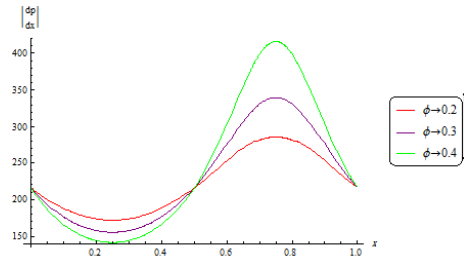


Figure 10- Variation of pressure gradient $\left| \frac{dp}{dx} \right|$ with respect to x for different values of ϕ with other parameters
 $\sigma = 4, M^2 = 5, \Omega = 0.5, F = -10, a = 0.2$,
 $y = 1, \mu = 0.4, \rho = 1.057, \lambda_1 = 0.2$

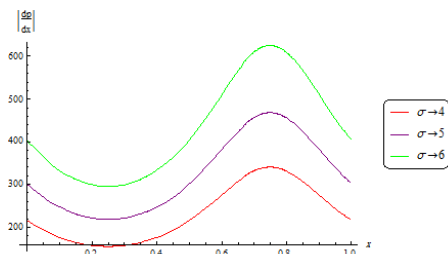


Figure 11- Variation of pressure gradient $\left| \frac{dp}{dx} \right|$ with respect to x for different values of σ with other parameters
 $\phi = 0.2, M^2 = 5, \Omega = 0.5, F = -10, a = 0.2$,
 $y = 1, \mu = 0.4, \rho = 1.057, \lambda_1 = 0.2$

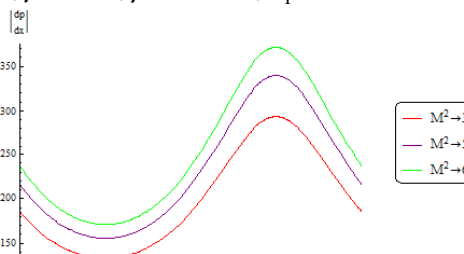


Figure 12- Variation of pressure gradient $\left| \frac{dp}{dx} \right|$ with respect to x for different values of M^2 with other parameters
 $\phi = 0.2, \sigma = 4, \Omega = 0.5, F = -10, a = 0.2$,
 $y = 1, \mu = 0.4, \rho = 1.057, \lambda_1 = 0.2$

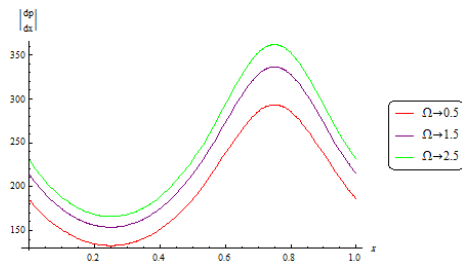


Figure 13- Variation of pressure gradient $\left| \frac{dp}{dx} \right|$ with respect to x for different values of Ω with other parameters

$$\phi = 0.2, M^2 = 5, \sigma = 4, F = -10, a = 0.2, y = 1, \mu = 0.4, \rho = 1.057, \lambda_1 = 0.2$$

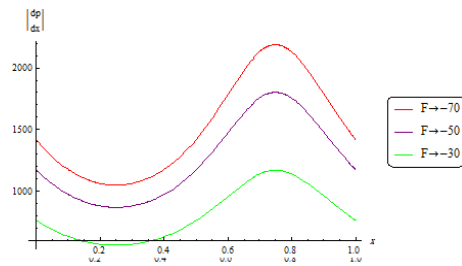


Figure 14- Variation of pressure gradient $\left| \frac{dp}{dx} \right|$ with respect to x for different values of F with other parameters

$$\phi = 0.2, M^2 = 5, \sigma = 4, \Omega = 0.5, a = 0.2, y = 1, \mu = 0.4, \rho = 1.057, \lambda_1 = 0.2$$

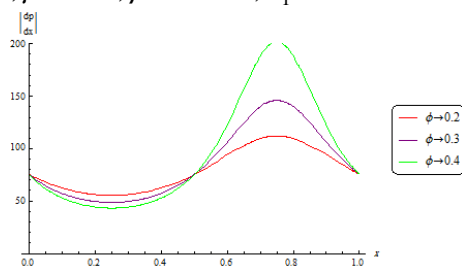


Figure 15- Variation of pressure gradient $\left| \frac{dp}{dx} \right|$ with respect to x for different values of ϕ with other parameters if $(\sigma^2 = 0)$

$$M^2 = 5, \Omega = 0.5, F = -10, a = 0.2, y = 1, \mu = 0.4, \rho = 1.057, \lambda_1 = 0.2$$

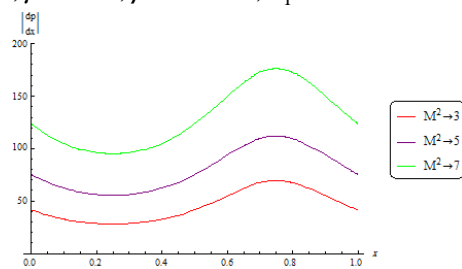


Figure 16- Variation of pressure gradient $\left| \frac{dp}{dx} \right|$ with respect to x for different values of M^2 with other parameters if $(\sigma^2 = 0)$

$$\phi = 0.2, \Omega = 0.5, F = -10, a = 0.2, y = 1, \mu = 0.4, \rho = 1.057, \lambda_1 = 0.2$$

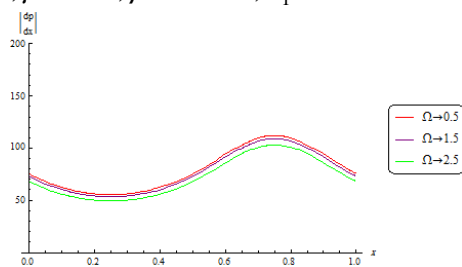


Figure 18- Variation of pressure gradient $\left| \frac{dp}{dx} \right|$ with respect to x for different values of Ω with other parameters if $(\sigma^2 = 0)$

$$\phi = 0.2, M^2 = 5, F = -10, a = 0.2, y = 1, \mu = 0.4, \rho = 1.057, \lambda_1 = 0.2$$

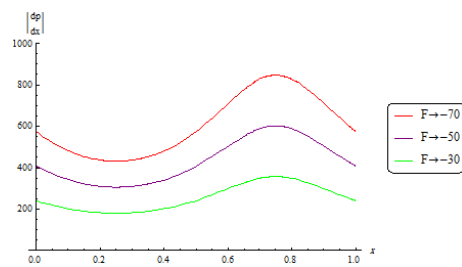


Figure 17- Variation of pressure gradient $\left| \frac{dp}{dx} \right|$ with respect to x for different values of F with other parameters if $(\sigma^2 = 0)$

$$\phi = 0.2, M^2 = 5, \Omega = 0.5, a = 0.2, y = 1, \mu = 0.4, \rho = 1.057, \lambda_1 = 0.2$$

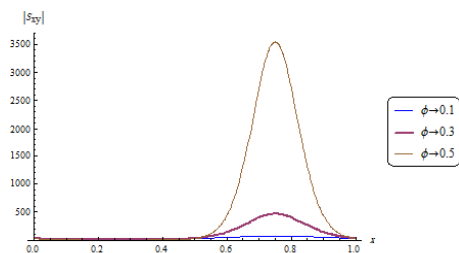


Figure 19- Variation of shear stress $|S_{xy}|$ with respect to x for different values of ϕ with other parameter $\sigma = 4, M^2 = 5, \Omega = 0.5, F = -10, a = 0.2, y = 1, \mu = 0.4, \rho = 1.057, \lambda_1 = 0.2$

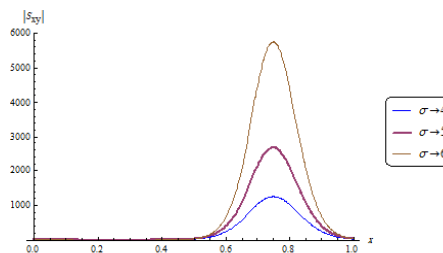


Figure 20- Variation of shear stress $|S_{xy}|$ with respect to x for different values of σ with other parameter $\phi = 0.2, M^2 = 5, \Omega = 0.5, F = -10, a = 0.2, y = 1, \mu = 0.4, \rho = 1.057, \lambda_1 = 0.2$.

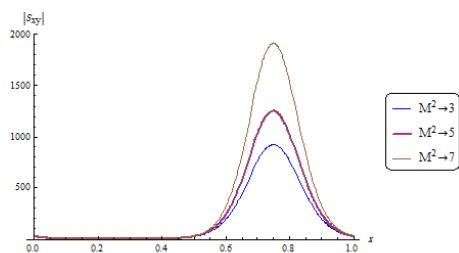


Figure 21- Variation of shear stress $|S_{xy}|$ with respect to x for different values of M^2 with other parameters $\phi = 0.2, \sigma = 4, \Omega = 0.5, F = -10, a = 0.2, y = 1, \mu = 0.4, \rho = 1.057, \lambda_1 = 0.2$

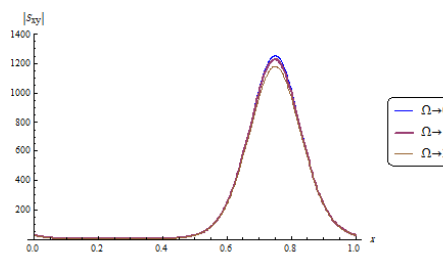


Figure 22- Variation of shear stress $|S_{xy}|$ with respect to x for different values of Ω with other parameters $\phi = 0.2, \sigma = 4, M^2 = 5, F = -10, a = 0.2, y = 1, \mu = 0.4, \rho = 1.057, \lambda_1 = 0.2$.

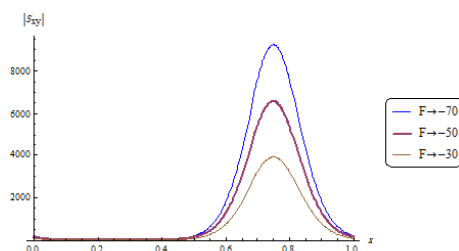


Figure 23- Variation of shear stress $|S_{xy}|$ with respect to x for different values of F with other parameters if $\phi = 0.2, \sigma = 4, M^2 = 5, \Omega = 0.5, a = 0.2, y = 1, \mu = 0.4, \rho = 1.057, \lambda_1 = 0.2$

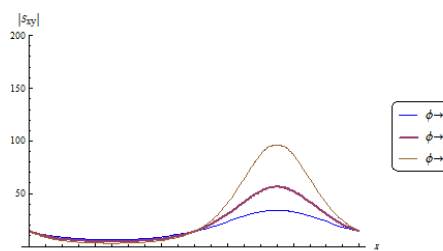


Figure 24- Variation of shear stress $|S_{xy}|$ with respect to x for different values of ϕ with other parameters if $(\sigma^2 = 0) M^2 = 5, \Omega = 0.5, F = -10, a = 0.2, y = 1, \mu = 0.4, \rho = 1.057, \lambda_1 = 0.2$.

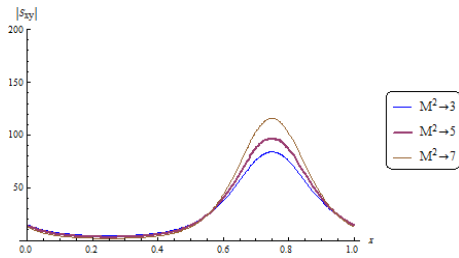


Figure 25- Variation of shear stress $|S_{xy}|$ with respect to x for different values of M^2 with other parameters if $(\sigma^2 = 0)$
 $\phi = 0.2, \Omega = 0.5, F = -10, a = 0.2,$
 $y = 1, \mu = 0.4, \rho = 1.057, \lambda_1 = 0.2$

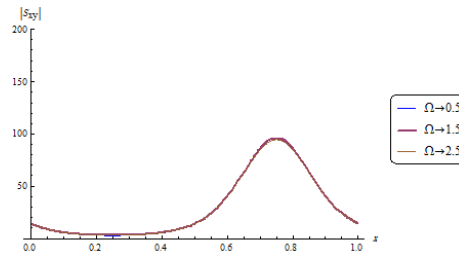


Figure 26- Variation of shear stress $|S_{xy}|$ with respect to x for different values of Ω with other parameters if $(\sigma^2 = 0)$
 $\phi = 0.2, M^2 = 5, F = -10, a = 0.2,$
 $y = 1, \mu = 0.4, \rho = 1.057, \lambda_1 = 0.2$

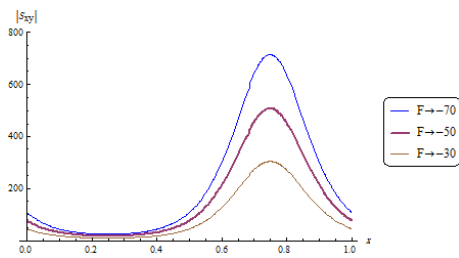


Figure 27- Variation of shear stress $|S_{xy}|$ with respect to x for different values of F with other parameters if $(\sigma^2 = 0)$
 $\phi = 0.2, M^2 = 5, \Omega = 0.5, a = 0.2,$
 $y = 1, \mu = 0.4, \rho = 1.057, \lambda_1 = 0.2$

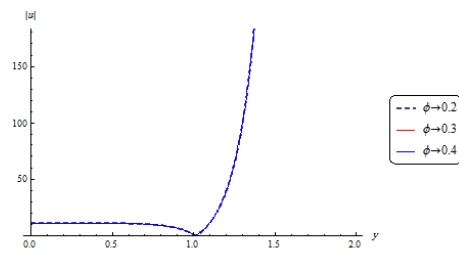


Figure 28- Variation of velocity $|u|$ with respect to y for different values of ϕ with other parameters
 $\sigma = 4, M^2 = 5, \Omega = 0.5, F = -10, a = 0.2,$
 $y = 1, \mu = 0.4, \rho = 1.057, \lambda_1 = 0.2 .$

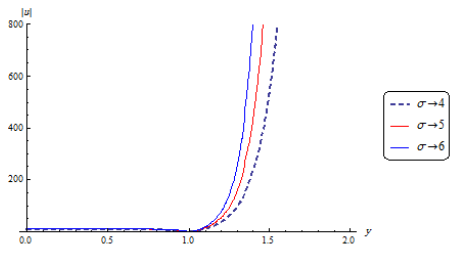


Figure 29- Variation of velocity $|u|$ with respect to y for different values of σ with other parameters
 $\phi = 0.2, M^2 = 5, \Omega = 0.5, F = -10, a = 0.2,$
 $y = 1, \mu = 0.4, \rho = 1.057, \lambda_1 = 0.2$

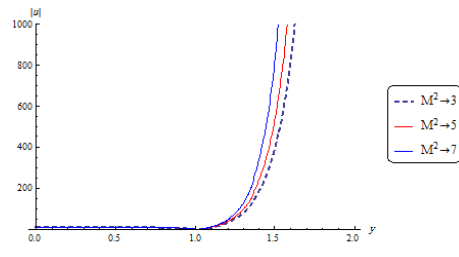


Figure 30- Variation of velocity $|u|$ with respect to y for different values of M^2 with other parameters
 $\phi = 0.2, \sigma = 4, \Omega = 0.5, F = -10, a = 0.2,$
 $y = 1, \mu = 0.4, \rho = 1.057, \lambda_1 = 0.2$

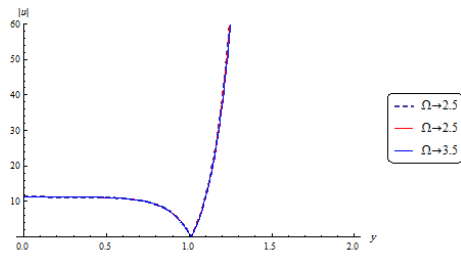


Figure 31- Variation of velocity $|u|$ with respect to y for different values of Ω with other parameters $\phi = 0.2, \sigma = 4, M^2 = 5, F = -10, a = 0.2, y = 1, \mu = 0.4, \rho = 1.057, \lambda_1 = 0.2$

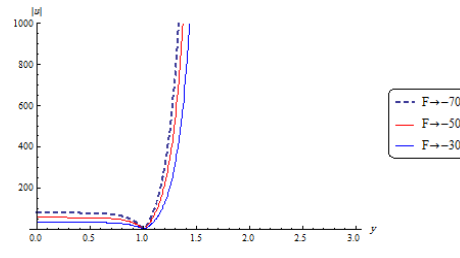


Figure 32- Variation of velocity $|u|$ with respect to y for different values of F with other parameters $\phi = 0.2, \sigma = 4, M^2 = 5, \Omega = 0.5, a = 0.2, y = 1, \mu = 0.4, \rho = 1.057, \lambda_1 = 0.2$

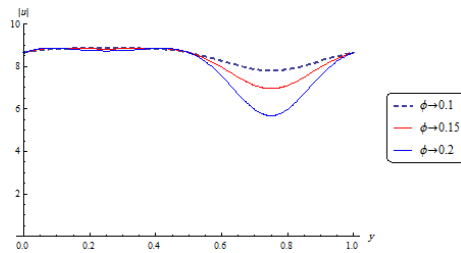


Figure 33- Variation of velocity $|u|$ with respect to y for different values of ϕ with other parameters if $(\sigma^2 = 0)$ $M^2 = 5, \Omega = 0.5, F = -10, a = 0.2, y = 1, \mu = 0.4, \rho = 1.057, \lambda_1 = 0.2$

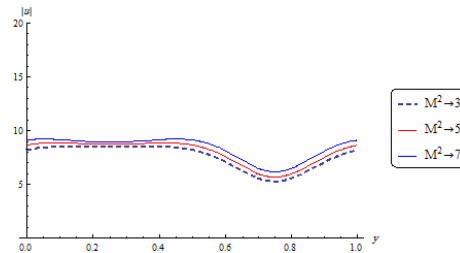


Figure 34- Variation of velocity $|u|$ with respect to y for different values of M^2 with other parameters if $(\sigma^2 = 0)$ $\phi = 0.2, \Omega = 0.5, F = -10, a = 0.2, y = 1, \mu = 0.4, \rho = 1.057, \lambda_1 = 0.2$.

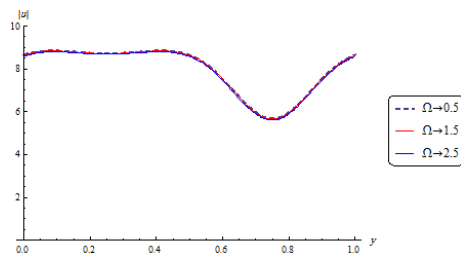


Figure 35- Variation of velocity $|u|$ with respect to y for different values of Ω with other parameters if $(\sigma^2 = 0)$ $\phi = 0.2, M^2 = 5, F = -10, a = 0.2, y = 1, \mu = 0.4, \rho = 1.057, \lambda_1 = 0.2$

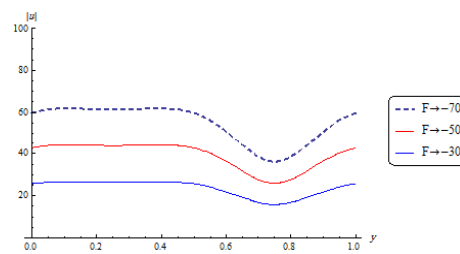


Figure 36- Variation of velocity $|u|$ with respect to y for different values of F other parameters if $(\sigma^2 = 0)$ $\phi = 0.2, M^2 = 5, \Omega = 0.5, a = 0.2, y = 1, \mu = 0.4, \rho = 1.057, \lambda_1 = 0.2$

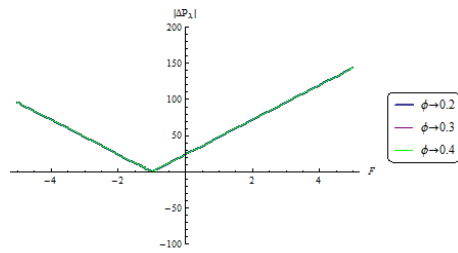


Figure 37- Variation of pressure rise $|\Delta P_\lambda|$ with respect to F for different values of ϕ with other parameters
 $\sigma = 4, M^2 = 5, \Omega = 0.5, x = 1, a = 0.2,$
 $y = 0.5, \mu = 0.4, \rho = 1.057, \lambda_1 = 0.2$

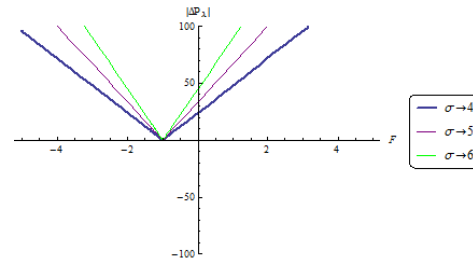


Figure 38- Variation of pressure rise $|\Delta P_\lambda|$ with respect to F for different values of σ with other parameters
 $\phi = 0.2, M^2 = 5, \Omega = 0.5, x = 1, a = 0.2,$
 $y = 0.5, \mu = 0.4, \rho = 1.057, \lambda_1 = 0.2.$

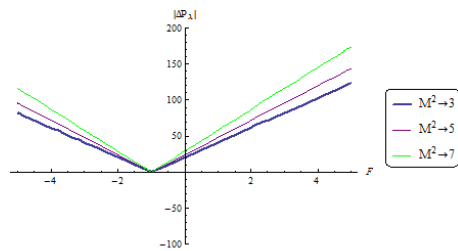


Figure 39- Variation of pressure rise $|\Delta P_\lambda|$ with respect to F for different values of M^2 with other parameters
 $\phi = 0.2, \sigma = 4, \Omega = 0.5, x = 1, a = 0.2,$
 $y = 0.5, \mu = 0.4, \rho = 1.057, \lambda_1 = 0.2$

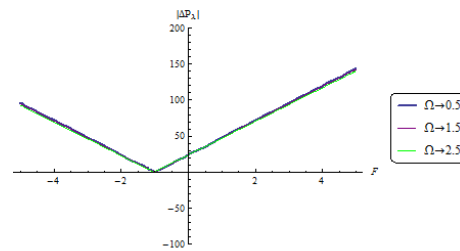


Figure 40- Variation of pressure rise $|\Delta P_\lambda|$ with respect to F for different values of Ω with other parameters
 $\phi = 0.2, \sigma = 4, M^2 = 5, a = 0.2,$
 $y = 0.5, \mu = 0.4, \rho = 1.057, \lambda_1 = 0.2, x = 1$

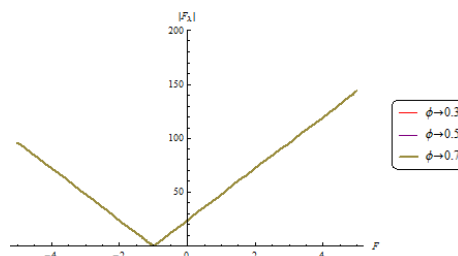


Figure 41- Variation of friction force $|F_\lambda|$ with respect to F for different values of ϕ with other parameters
 $\Omega = 0.5, \sigma = 4, M^2 = 5, a = 0.2,$
 $y = 0.5, \mu = 0.4, \rho = 1.057, \lambda_1 = 0.2, x = 1$

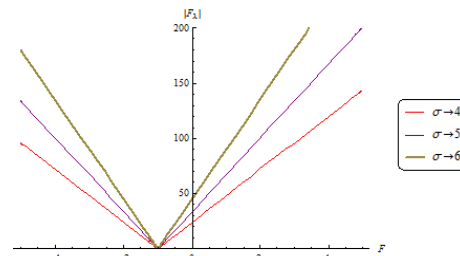


Figure 42- Variation of friction force $|F_\lambda|$ with respect to F for different values of σ with other parameters
 $\Omega = 0.5, \phi = 0.2, M^2 = 5, a = 0.2,$
 $y = 0.5, \mu = 0.4, \rho = 1.057, \lambda_1 = 0.2, x = 1$

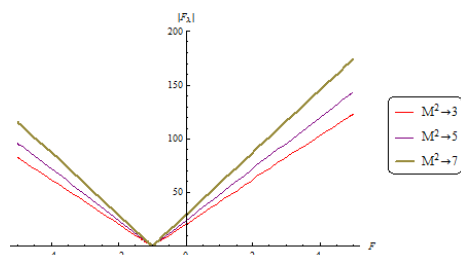


Figure 43- Variation of friction force $|F_\lambda|$ with respect to F for different values of M^2 with other parameters $\Omega = 0.5, \phi = 0.2, \sigma = 4, a = 0.2, y = 0.5, \mu = 0.4, \rho = 1.057, \lambda_1 = 0.2, x = 1$

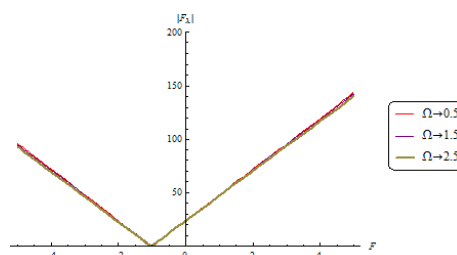


Figure 44- Variation of friction force $|F_\lambda|$ with respect to F for different values of Ω with other parameters $M^2 = 5, \phi = 0.2, \sigma = 4, a = 0.2, y = 0.5, \mu = 0.4, \rho = 1.057, \lambda_1 = 0.2, x = 1$

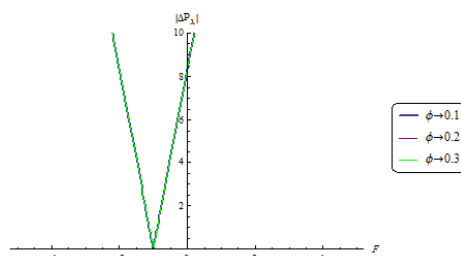


Figure 45- Variation of pressure rise $|\Delta P_\lambda|$ with respect to F for different values of ϕ with other parameters if $(\sigma^2 = 0)$ $M^2 = 5, \Omega = 0.5, x = 1, a = 0.2, y = 0.5, \mu = 0.4, \rho = 1.057, \lambda_1 = 0.2$

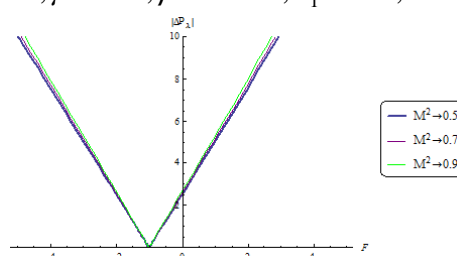


Figure 46- Variation of pressure rise $|\Delta P_\lambda|$ with respect to F for different values of M^2 with other parameters if $(\sigma^2 = 0)$ $\phi = 0.2, \Omega = 0.5, x = 1, a = 0.2, y = 0.5, \mu = 0.4, \rho = 1.057, \lambda_1 = 0.2$.

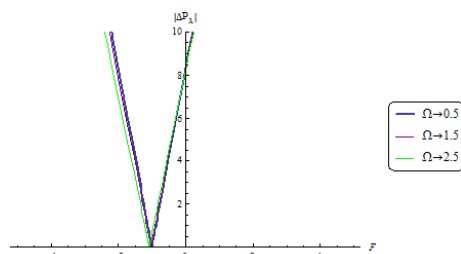


Figure 47- Variation of pressure rise $|\Delta P_\lambda|$ with respect to F for different values of Ω with other parameters if $(\sigma^2 = 0)$ $\phi = 0.2, M^2 = 5, a = 0.2, y = 0.5, \mu = 0.4, \rho = 1.057, \lambda_1 = 0.2, x = 1$

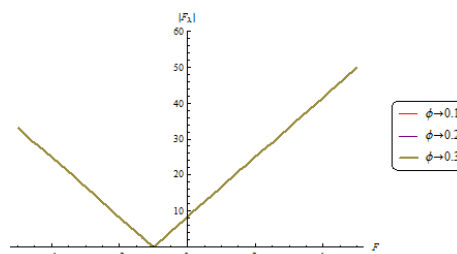


Figure 48- Variation of friction force $|F_\lambda|$ with respect to F for different values of ϕ $\Omega = 0.5, M^2 = 5, a = 0.2, y = 0.5, \mu = 0.4, \rho = 1.057, \lambda_1 = 0.2, x = 1$

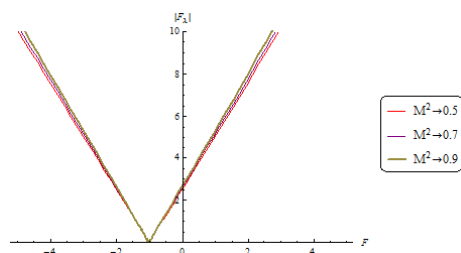


Figure 49- Variation of friction force $|F_\lambda|$ with respect to F for different values of M^2 with other parameters if $(\sigma^2 = 0)$
 $\Omega = 0.5, \phi = 0.2, a = 0.2,$
 $y = 0.5, \mu = 0.4, \rho = 1.057, \lambda_1 = 0.2, x = 1$

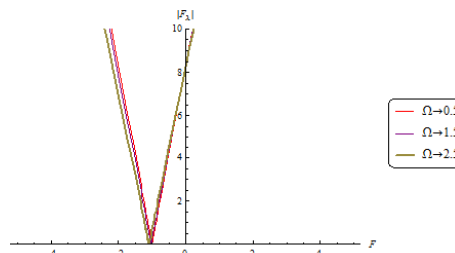


Figure 50- Variation of friction force $|F_\lambda|$ with respect to F for different values of Ω with other parameters if $(\sigma^2 = 0)$
 $M^2 = 5, \phi = 0.2, a = 0.2,$
 $y = 0.5, \mu = 0.4, \rho = 1.057, \lambda_1 = 0.2, x = 1$

10. Conclusion

The influence of rotation and magnetic field on the nonlinear peristaltic flow of a Jeffery fluid in an asymmetric channel through a porous medium has been analyzed. The analytical expressions are constructed for the stream function, pressure gradient, pressure rise, fractional force, shear stress and velocity. The main findings of the present study are given in following points:

1. The absolute value of stream function decreases with increasing rotation and dimensionless time-mean flow, while it increases with increasing non-dimensional wave amplitude, the porosity and Hartman number. But when the porosity σ is neglected the absolute value of stream function decreases with increasing dimensionless time-mean flow, while it increases with increasing non-dimensional wave amplitude, Hartman number and rotation.
2. The absolute value of pressure gradient decreases with increasing dimensionless time-mean flow, while it increases with increasing non-dimensional wave amplitude, the porosity, Hartman number and rotation. But when the porosity σ is neglected the absolute value of pressure gradient decrease with increasing dimensionless time-mean flow and rotation, while it increases with increasing non-dimensional wave amplitude and Hartman number.
3. The absolute value of shear stress decreases with increasing dimensionless time-mean flow and rotation, while it increases with increasing non-dimensional wave amplitude, the porosity and Hartman number. But when the porosity σ is neglected the absolute value of shear stress decreases with increasing dimensionless time-mean flow and rotation, while it increases with increasing non-dimensional wave amplitude and Hartman number.
4. The absolute value of velocity decreases with increasing dimensionless time-mean flow and rotation, while it increases with increasing non-dimensional wave amplitude, the porosity and Hartman number, and when the porosity is σ neglected we obtain the absolute value of velocity decreases with increasing dimensionless time-mean flow, rotation and wave amplitude, while it increases with increasing Hartman number.
5. The absolute value of pressure rise and the absolute value of friction force decreases with increasing rotation, while it increases with increasing non-dimensional wave amplitude, the porosity and Hartman and the $|\Delta P_\lambda|$ number. And when the porosity σ is neglected it is observed that the absolute value of pressure rise and the absolute value of friction force increase with increasing non-dimensional wave amplitude and Hartman number, while they decrease with increasing rotation.

References

1. Abd-Alla A.M., Abo-Dahab S.M. and El-Shahrany H. D. **2013**. Effects of rotation and magnetic field on the nonlinear peristaltic flow of a second-order fluid in an asymmetric channel through a porous medium, *Chinese Physics B*, 22,pp:1-10.
2. Scheidgger, A.E. **1963**. *The physics of flow through a porous media*. University of Toronto Press.
3. Srinivas, S. and Gayathri, R. **2009**. Peristaltic transport of a Newtonian fluid in a vertical asymmetric channel with heat transfer and porous medium, *Applied Mathematics and Computation*, 215, pp:185-196.
4. Kothandapani, M. and Srinivas ,S. **2008**. Peristaltic transport of a Jeffery fluid under the effect of magnetic field in an asymmetric channel, *Physics Letter A*, 372, pp:4586-4591.
5. Mahmoud S. R., Afifi N. A. S. and Al-Isede H. M. **2011**. Effect of porous medium and magnetic field on the peristaltic transport of a Jeffery fluid, *Journal of Math Analysis*, 5, pp:1025-1034.
6. Abd-Alla A.M. and Abo-Dahab S.M. **2015**. Magnetic field and rotation effects on the peristaltic transport of a Jeffery fluid in an asymmetric channel, *Journal of Magnetism and Magnetic Materials*, 374, pp:680-689.
7. Nadeem S., Arshad riaz and Ellahi R. **2013**. Peristaltic flow of a Jeffery fluid in rectangular duct having compliant walls, *Chemical Industry and Chemical Engineering Quarterly*, 19, pp:399-409.
8. Mahmoud S.R., Abd-alla A.M. and El-sheikh M.A. **2011**. Effect of the rotation on wave motion through cylindrical bore in a micro-polar porous medium, *International Modern Physics B*, 25, pp:2712-2728.